Finite band inversion of angular-resolved photoemission in $Bi_2Sr_2CaCu_2O_{8+\delta}$ and comparison with optics

E. Schachinger[1,*] and J. P. Carbotte[2,3]
[1]*Institute of Theoretical and Computational Physics, Graz University of Technology, A-8010 Graz, Austria*
[2]*Department of Physics and Astronomy, McMaster University, Hamilton, Ontario, Canada L8S 4M1*
[3]*Canadian Institute for Advanced Research, Toronto, Ontario, Canada M5G 1Z8*
(Received 27 December 2007; published 31 March 2008)

Using a maximum entropy technique within a finite band Eliashberg formalism, we extract from recent high accuracy nodal direction angular-resolved photoemission spectroscopy data in optimally doped $Bi_2Sr_2CaCu_2O_{8+\delta}$ (Bi2212) a quasiparticle electron-boson spectral density. Both normal and superconducting states with *d*-wave gap symmetry are treated. Finite and infinite band results are considered and contrasted. We compare with results obtained for the related transport spectral density, which follows from a similar inversion of optical data. We discuss the implication of our results for quasiparticle renormalizations in the antinodal direction.

DOI: 10.1103/PhysRevB.77.094524 PACS number(s): 74.20.Mn, 74.25.Gz, 74.72.−h

I. INTRODUCTION

Maximum entropy techniques have proved useful in attempts to extract boson information either from angular-resolved photoemission spectroscopy (ARPES) data or from the optical conductivity.[1–5] What is recovered is the electron-boson spectral density, $I^2\chi(\omega)$, which describes the effective interaction between two electrons due to the exchange of a boson which could be a phonon, a spin fluctuation, or some other excitation such as a plasmon. In this way, one can obtain some insight into the nature of this interaction and by implication about the mechanism of superconductivity. In particular, coupling to a resonance peak in $I^2\chi(\omega)$ can lead to peaks or kinks in measured quantities. As we will see, even a structureless background can be picked up in our inversion process. Other approaches to the analysis of such structures have also been applied; see, for example, Mishchenko and Nagaosa[6] who employed the *t-J* model.

ARPES gives information on the quasiparticle self-energy while optical data can be expressed in terms of an optical self-energy which is related to, but is different from, the quasiparticle self-energy. There are two main differences. The first is that optics involves the current-current correlation function which can be expressed in terms of a two-particle Green's function and there can be vertex corrections while ARPES requires only the knowledge of the one-particle Green's function. Optics deals with a transport process and transport lifetimes are not the same as quasiparticle lifetimes. For example, the effectiveness of a scattering process in depleting a current depends strongly on the final state, i.e., backward as opposed to forward scattering. Second, optics deals with a momentum average while ARPES is momentum specific. There are other complications: ARPES measures renormalized quasiparticle energies directly and to extract from this data the quasiparticle self-energy it is necessary to know the bare dispersion relation. Often, for energies not too far from the chemical potential, a linear dispersion is assumed and its slope is determined from an assumption that the self-energy crosses zero at some energy ~400 meV in the recent high accuracy data in $Bi_2Sr_2CaCu_2O_{8+\delta}$ (Bi2212).[7] A similar ambiguity arises in optics: To get the optical self-energy from the reflectivity data, it is necessary to specify a value for the dielectric constant ε at infinity. Also, the plasma frequency is needed and this quantity is not so well known in the cuprates. In some determination, it requires an assumption about where the band of interest ends as there are overlaps with higher bands, creating ambiguity.

Certainly, we are dealing with a finite band situation. For a simple first neighbor only tight binding band with hoping t, the bandwidth $W=8t$. Estimates based on tight binding fits to local density approximation (LDA) band structure calculations give values of the order of 350–450 meV[8] for t while fits to experiment can give somewhat smaller values of order 200 meV. In all cases, of course, higher nearest neighbor hoping is also present.

So far, maximum entropy inversion techniques have involved using as an effective low energy theory for the self-energy the Eliashberg equation generalized to include any boson-exchange mechanism and not just phonons. However, these are written for infinite bands. A deficiency of such an approach is that the self-energy cannot change sign in an infinite band nor can its optical counterpart. On the other hand, in finite band formulations a change of sign occurs naturally and is a robust feature of the formulation.[9,10] In early ARPES experiments, the real part of the quasiparticle self-energy was simply assumed to go to zero at ~300 meV. In the work of Meevasana *et al.*[11] for the $La_{2-x}Sr_xCuO_4$ series, the renormalized dispersions were found to cross the bare LDA bands at most dopings considered, with the energy of the crossing falling roughly in the range of 400–600 meV. Furthermore, in the Bi2212 series of Hwang *et al.*,[12] the optical self-energy was also found to go through zero. On the theoretical side, Cappelutti and Pietronero[10] noted that in an electron-phonon model the real part of the self-energy always goes through a zero at some finite energy. Later, Knigavko and Carbotte[9] established that for coupling to an Einstein mode the zero occurs at $\sim\sqrt{\omega_E W/2}$ where ω_E is the frequency of the oscillator. For optics, the crossing is at higher energies, $\sim\sqrt{2}$ times its quasiparticle counterpart to logarithmic accuracy.

In this paper, we start by generalizing the maximum entropy inversion technique for the quasiparticle self-energy used by Shi *et al.*[3] to finite bands. We use this formalism to study how the value of the bandwidth W changes results obtained for the electron-boson spectral density $I^2\chi(\omega)$. First, we consider the normal state and generalize the procedure later on to deal with superconductivity. For this purpose, it is necessary to have finite W Eliashberg equations with d-wave symmetry for the superconducting gap. We use these equations to derive from the data of Zhang *et al.*[7] the spectral functions $I^2\chi(\omega)$ at low temperatures in the superconducting state. The available data are for the nodal direction only. In principle, the spectral density depends on direction and so antinodal results would be expected to be different. On the other hand, optics involves a transport spectral density, which is an average over all directions in momentum space. While this means that ARPES and optics cannot be compared directly,[13] we, nevertheless, use the spectral density $I^2\chi(\omega)_{\mathrm{tr}}$ taken from the optical literature to get some approximate information on a quantity which should be close to the angular averaged quasiparticle self-energy. We comment on the points of agreement as well as the disagreements that are found.

In Sec. II, we provide details of our formalism and describe results for the normal state. Section III deals with the superconducting state and also provides a comparison with optics. Finally, Sec. IV gives a brief summary and conclusions. Mathematical details are found in the Appendix.

II. FORMALISM: NORMAL STATE

Maximum entropy techniques can be used to extract a spectral function $I^2\chi(\omega)$ from the knowledge of the quasiparticle self-energy $\Sigma(\omega+i\delta)$ related in integral form through a known kernel $K(\omega,\nu)$ (specified below), namely,

$$\Sigma(\omega+i\delta)=\int_{-\infty}^{\infty}d\nu\,K(\omega+i\delta,\nu)I^2\chi(\nu), \tag{1}$$

where $I^2\chi(\omega)$ is the electron-boson spectral density which describes the interaction of two electrons by the exchange of a boson of energy ν. The kernel $K(\omega,\nu)$ is within Eliashberg theory in the normal state[9,14–19]

$$K(\omega+i\delta,\nu)=\int_{-\infty}^{\infty}d\omega'\frac{\tilde{N}(\omega')}{N_0(0)}\left[\frac{n(\nu)+f(-\omega')}{\omega-\nu-\omega'+i\delta}+\frac{n(\nu)+f(\omega')}{\omega+\nu-\omega'+i\delta}\right]. \tag{2}$$

Here, $\tilde{N}(\omega')$ is the fully renormalized electronic density of states and carries the information on finite band effects, $f(\omega)$ and $n(\nu)$ are the Fermi and Bose distribution functions, and δ is an infinitesimal positive parameter. For infinite bands, $\tilde{N}(\omega)\equiv N_0(0)$ and $K(\omega+i\delta,\nu)$ reduces to a closed form. Here, $N_0(0)$ is the bare electronic density of states at the Fermi energy taken to be a constant.

It is clear that both real and imaginary parts of $\Sigma(\omega+i\delta)$ are related to the desired spectral function through a convolution integral to which maximum entropy techniques apply and either can be used. Inversion of self-energy data on $\Sigma(\omega+i\delta)$ in finite bands requires additional information on $\tilde{N}(\omega)$. This complication, however, can easily be handled. The quasiparticle spectral density $A(\mathbf{k},\omega)$ is related to the one-particle Green's function $G(\mathbf{k},\omega)$ by

$$A(\mathbf{k},\omega+i\delta)=-\frac{1}{\pi}\,\mathrm{Im}\{G(\mathbf{k},\omega+i\delta)\}, \tag{3}$$

with Dyson's equation

$$G(\mathbf{k},\omega+i\delta)=\frac{1}{\omega+i\delta-\varepsilon_{\mathbf{k}}-\Sigma(\omega+i\delta)}, \tag{4}$$

where $\varepsilon_{\mathbf{k}}$ is the bare electron dispersion relation. For isotropic bands, we can use $\varepsilon=\varepsilon(\mathbf{k})$ to label the states instead of momentum and take the simplest finite band model for the bare density of states $N_0(\varepsilon)=1/W$ for ε in the interval $[-W/2,W/2]$ and zero otherwise. The renormalized quasiparticle density of states is then

$$\tilde{N}(\omega)=\int_{-\infty}^{\infty}d\varepsilon N_0(\varepsilon)A(\varepsilon,\omega)=-\frac{1}{\pi}\int_{-W/2}^{W/2}d\varepsilon N_0(0)\mathrm{Im}\left\{\frac{1}{\omega+i\delta-\varepsilon-\Sigma(\omega+i\delta)}\right\}. \tag{5}$$

Let us assume we know $\Sigma(\omega+i\delta)$ by some means, then $\tilde{N}(\omega)$ is known from Eq. (5) and the kernel equation (2) for the maximum entropy inversion is now definite and the procedure can be carried out.

ARPES experiments usually provide information only on the real part of the quasiparticle self-energy, $\Sigma_1(\omega)$. Thus, we separate Eq. (1) into its real and imaginary parts and apply the maximum entropy method to deconvolute only

$$\Sigma_1(\omega)=\int_{-\infty}^{\infty}d\nu\,K(\omega,\nu)I^2\chi(\nu), \tag{6}$$

with the kernel

$$K(\omega,\nu)=\int_{-\infty}^{\infty}\mathcal{P}d\omega'\frac{\tilde{N}(\omega')}{N_0(0)}\left[\frac{n(\nu)-f(-\omega')}{\omega-\nu-\omega'}+\frac{n(\nu)+f(\omega')}{\omega+\nu-\omega'}\right]. \tag{7}$$

Here, $\mathcal{P}$ indicates that a principal part integral is to be taken. Equation (7) differs from the one suggested by Shi *et al.*[3] in their inversion work in two regards. It contains the fully renormalized density of states $\tilde{N}(\omega)$ which accounts for finite band effects and the Bose distribution function $n(\nu)$ is included because we do not want to be restricted to the low temperature range.

If the imaginary part of the self-energy, $\Sigma_2(\omega)$, is not known from experimental data, Eq. (5) cannot be applied directly to calculate $\tilde{N}(\omega)$ and it is, therefore, required to develop an iterative, self-consistent formalism which will in the end allow us to extract the desired spectral function $I^2\chi(\omega)$ in the finite band case from $\Sigma_1(\omega)$ alone. As the ker-

nel (7) is based on Eliashberg theory, it is only natural to use the set of finite band d-wave Eliashberg equations,[20–23] as they are given in the Appendix, to calculate $\Sigma(\omega)$ for a given temperature T and a given spectral function $I^2\chi(\omega)$. When this is done, the normalized quasiparticle density of states $\tilde{N}(\omega)$ of Eq. (5) can be evaluated for any choice of spectral density. The following self-consistent procedure can be established: (1) An assumption is made for $\tilde{N}(\omega)$ and the simplest one, namely, $\tilde{N}(\omega)/N_0(0)=1/W$ in the interval $[-W/2,W/2]$ will suffice. Here, W is the bandwidth. (2) Equation (6) is deconvoluted using maximum entropy techniques and the experimental data on $\Sigma_1(\omega)$ for a given temperature T. In this step, it is necessary to adjust W, which is an external parameter to the deconvolution, as is $\tilde{N}(\omega)$, for best data reproduction. The result is a first approximation to the desired spectral function $I^2\chi(\omega)$. (3) A solution of the finite band d-wave Eliashberg equations (A1a)–(A1h) based on this approximate function $I^2\chi(\omega)$, the assumed value of W, and the given temperature T is generated. From this solution, the complex quasiparticle self-energy $\Sigma(\omega)$ is easily calculated and Eq. (5) can be solved to give a new fully renormalized density of states $\tilde{N}(\omega)$ and the procedure returns to step (1) until self-consistency is reached. Another possibility is to start with steps (1) and (2) from above. The approximate solution for $I^2\chi(\omega)$ can then be parametrized and a least squares fit procedure using the finite band d-wave Eliashberg equations (A1a)–(A1h) can be employed to get the best fit to the experimental $\Sigma_1(\omega)$ even when the data are taken in the superconducting state. This is our preferred method.

To get some understanding of how important finite band effects might be in maximum entropy inversions of the quasiparticle self-energy data, we proceed as follows. Hwang *et al.*[5] have obtained from optical conductivity data results for the average transport spectral function $I^2\chi(\omega)_{\rm tr}$ in Bi2212 as a function of temperature and doping. The solid curve of Fig. 1 reproduces their results for an overdoped sample (T_c =82 K, labeled BI82B) at T=26 K. This function is used in Eqs. (6) and (7) with $W\to\infty$ so that $\tilde{N}(\omega')/N_0(0)=1$, to obtain the real part of the quasiparticle self-energy of Eq. (1). [We will refer to it as the input $I^2\chi(\omega)$.] Next, the procedure is reversed and maximum entropy techniques are used to derive from these numerical data a new spectral function $I^2\chi(\omega)$ which is shown as the dashed curve in Fig. 1 and which is seen to be almost identical to the input curve as it must be. Next, we compute again $\Sigma_1(\omega)$ from the same input $I^2\chi(\omega)$ but now we apply a finite band cutoff to the normal state version of the Eliashberg equations (A1a)–(A1h) to generate a new set of numerical $\Sigma_1(\omega)$ data. This new set is again used as input for a maximum entropy infinite band deconvolution of Eq. (6) to yield a new model $I^2\chi(\omega)$. Results of this procedure for W=2.5 eV (dotted curve) and W =1.25 eV (dash-dotted curve) are given in Fig. 1. It is seen that the application of a finite band cutoff to the calculation of $\Sigma_1(\omega)$ has a major effect at energies beyond 100 meV where the new $I^2\chi(\omega)$ is considerably reduced over its input value. This was to be expected since inverting in an infinite band model does not account for the reduction in self-energy

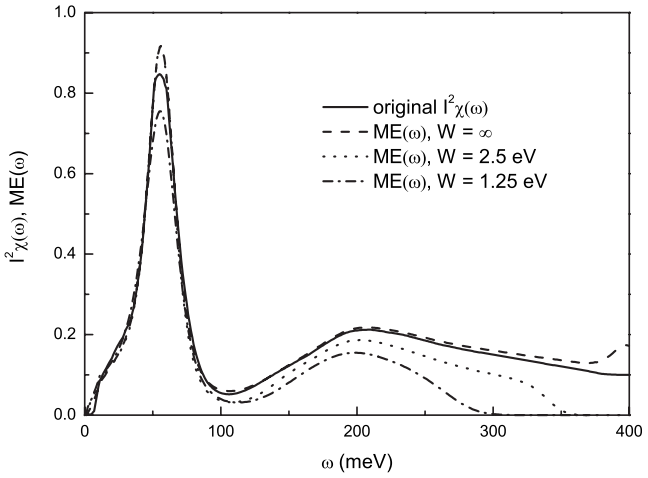

FIG. 1. The electron-boson spectral density $I^2\chi(\omega)$ recovered from inversion of the real part of the quasiparticle self-energy calculated with common $I^2\chi(\omega)$ (solid curve) but with different bandwidths $W=\infty$ (dashed), W=2.5 eV (dotted), and W=1.25 eV (dash dotted). In all cases, the inversion was carried out assuming an infinite band.

that is brought about by the decay in the effective electronic density of states around the bare band edge and beyond. It is clear that to do realistic inversions in the cuprates, finite band effects need be accounted for. This is also required if the real part of the quasiparticle self-energy is to cross zero at some finite energy, say, 400 meV, as was assumed in the analysis of the experimental data of Zhang *et al.*[7] On the other hand, if one is mainly interested in the small energy region much less than the zero crossing at ~400 meV, finite band effects make little difference except for lowering somewhat the peak around 60 meV in comparison to our input spectral function.

Having established our inversion technique, we next go to experiments. We started with the T=99 K data from Fig. 4(a) of Ref. 7 and inverted it according to Eqs. (6) and (7) to recover the electron-boson spectral function $I^2\chi(\omega)$ in the specific case of the nodal direction at 99 K in the normal state. Results are presented in Fig. 2. Two different values of the bandwidth, namely, W=1.2 eV (solid curve) and 2.0 eV (dashed curve) were used together with $W=\infty$ (dotted curve). In all cases, the same experimental data appear on the left hand side of Eq. (6). For the dashed and dotted curves, bandwidths W=2 eV and $W=\infty$, respectively, were imposed on the inversion procedure from the outside. For the solid curve, the parameter W was allowed to vary. Instead, a constraint, namely, that the resulting self-energy $\Sigma_1(\omega)$ be zero exactly at ω=400 meV, was applied. This resulted in a value W =1.2 eV. Of course, it needs to be recognized that the ARPES experiments themselves do not tell us where the zero in $\Sigma_1(\omega)$ occurs. Some assumption on the bare dispersion is needed and the value 400 meV while respected in our inversions for the solid curve is, therefore, model dependent. If one had an independent, reliable estimate of the bandwidth, then this value could be used as a constraint in the inversion and this would yield an estimate of the energy at which renormalized and bare band dispersions meet. Returning to Fig. 2, it should now be clear why for a fixed set of $\Sigma_1(\omega)$

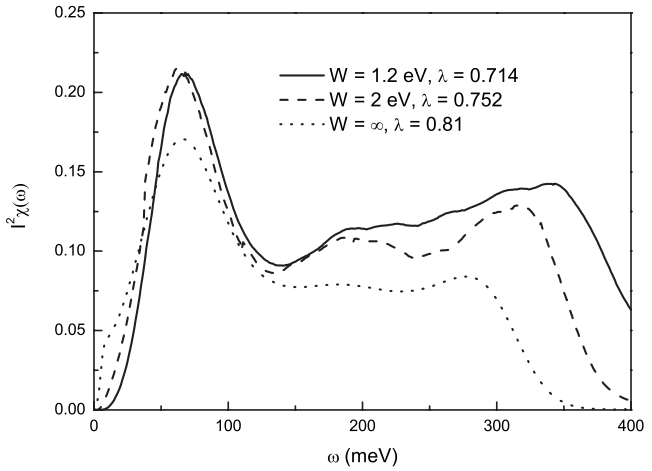

FIG. 2. Result for the electron-boson spectral density $I^2\chi(\omega)$ obtained from inversion of the ARPES nodal direction Bi2212 data at $T=99$ K of Zhang *et al.* (Ref. 7). The dotted curve is for an infinite band, the dashed one for a bandwidth $W=2$ eV, and the solid one for $W=1.2$ eV. Note the reduction of spectral weight beyond ~100 meV as W is increased. Values of the mass enhancement factor are 0.81, 0.752, and 0.714, respectively.

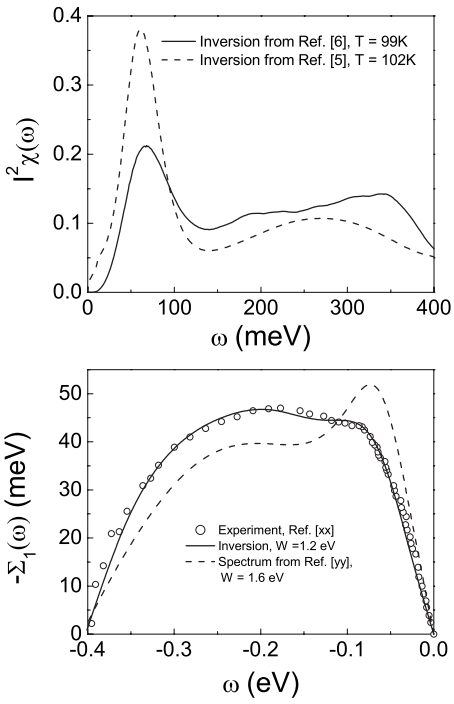

FIG. 3. Top frame: Electron-boson spectral density $I^2\chi(\omega)$ from finite band inversion ($W=1.2$ eV) of ARPES data in nodal direction (Ref. 7) in the normal state at $T=99$ K (solid curve). The dashed curve is for comparison and was obtained previously by the inversion of optical data (Ref. 5) and scaled down by a factor of 0.44 so as to account for differences between quasiparticle and transport quantities. Bottom frame: Real part of the quasiparticle energy at $T=99$ K in the normal state. The open circles are the data of Zhang *et al.* (Ref. 7) as read off their Fig. 4(a). The solid curve represents the result of the maximum entropy inversion of the data assuming a bandwidth of $W=1.2$ eV so as to get a zero in the self-energy at ~400 meV as in the experimental data. The dashed curve was obtained using the $I^2\chi(\omega)$ shown by a dashed line in the top frame. A bandwidth of 1.6 eV was chosen to, again, give a zero in $\Sigma_1(\omega)$ at ~400 meV.

data increasing the value of W leads to smaller values of $I^2\chi(\omega)$ at higher energies. Renormalization effects in this region can be reduced due to a smaller value of $I^2\chi(\omega)$ which, in turn, results in a reduced quasiparticle density of states. Finally, we note that the mass renormalization value $\lambda = 2\int_0^\infty d\omega\, I^2\chi(\omega)/\omega$ is of the order 0.7–0.8 for optimally doped Bi2212. These values are considerably smaller than those determined from optics as we will discuss later. There appears to be a factor of 2 difference in the magnitude between quasiparticle and transport electron-boson spectral density.

Our best fit for $I^2\chi(\omega)$ to the data of Ref. 7 is reproduced as the solid curve in the top frame of Fig. 3 where it is compared with data on $I^2\chi(\omega)_{\rm tr}$ (dashed curve) which was obtained from maximum entropy inversions of optical data by Hwang *et al.*[5] for a similar optimally doped Bi2212 sample. A scaling factor of 0.44 was applied to $I^2\chi(\omega)_{\rm tr}$ in this case. The resulting mass enhancement $\lambda=1.09$, which is to be compared with the value of 0.72 we found from ARPES. The above scaling factor was determined in an attempt to get the best possible agreement to the ARPES quasiparticle self-energy $\Sigma_1(\omega)$ without changing the shape of $I^2\chi(\omega)_{\rm tr}$. The corresponding self-energy is shown as a dashed line in the bottom frame of Fig. 3. The solid curve derived from ARPES data, of course, fits data very well within the considered energy range of $[-0.4\ \text{eV}, 0]$ for the experimental data of Ref. 7, which are indicated by open circles. The dashed curve calculated from the rescaled $I^2\chi(\omega)_{\rm tr}$ (dashed line in the top frame of Fig. 3) shows remarkable similarity. The main difference is due to the fact that the peak in $I^2\chi(\omega)_{\rm tr}$ from optics at 62 meV is stronger than the one in the ARPES data, which is at 68 meV. This is not unexpected since optics produces an electron-boson spectral density which is an average over all momenta while ARPES is momentum specific, namely, **k** is in the nodal direction. If we associate the peak with the interaction of the charge carriers with some spin fluctuations peak around (π,π) in the two-dimensional CuO Brillouin zone then we would expect this peak to be larger for scattering in the antinodal direction and, therefore, larger in the average function of optics than in the nodal function of ARPES.

The good agreement found here between the ARPES and optics derived spectral density noted in the top frame of Fig. 3 shows that both methods agree that there is a strong coupling to an excitation at $\omega=60$ meV as well as a high energy background which extends to 400 meV. This cannot be due to phonons but finds a natural interpretation as coupling to spin fluctuations.

III. SUPERCONDUCTING STATE AND RESULTS BASED ON OPTICS

In the superconducting state, the basic inversion procedure outlined in the previous section is no longer applicable

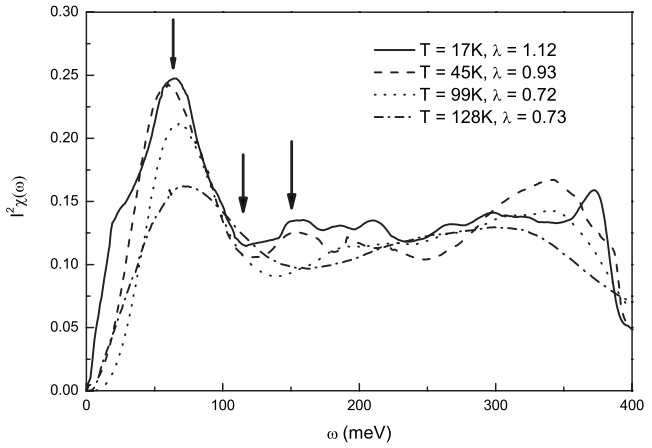

FIG. 4. Results for the electron-boson spectral density $I^2\chi(\omega)$ obtained by inversion of ARPES data by Zhang *et al.* (Ref. 7) along the nodal direction at different temperatures, namely, $T=128$ K (dash-dotted line, $\lambda=0.73$), $T=99$ K (dotted line, $\lambda=0.72$), $T=45$ K (dashed line, $\lambda=0.93$, superconducting state), and $T=17$ K (solid line, $\lambda=1.12$, superconducting state). A finite bandwidth $W=1.2$ eV was applied.

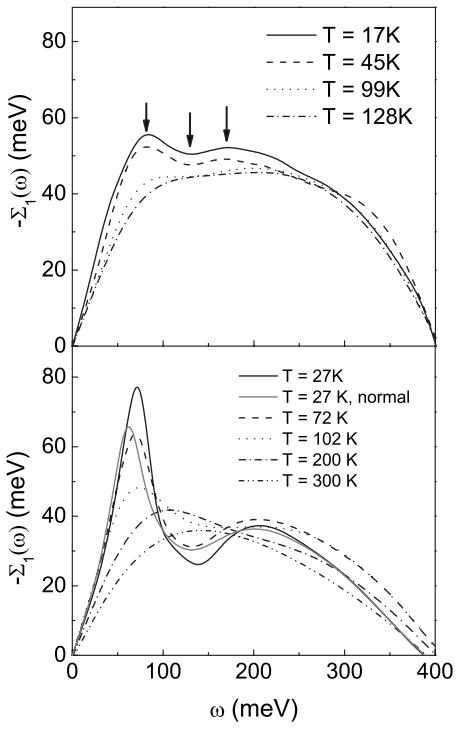

FIG. 5. Top frame: The self-energy $\Sigma_1(\omega)$ vs ω calculated from the spectral densities shown in Fig. 4, which have been found from inversion of ARPES data reported by Zhang *et al.* (Ref. 7). A finite bandwidth of $W=1.2$ eV was applied. Bottom frame: The self-energy $\Sigma_1(\omega)$ vs ω calculated from electron-boson spectral densities $I^2\chi(\omega)$ obtained from optics (Ref. 5) and scaled by a factor of 0.44. A finite bandwidth $W=1.6$ eV was applied.

because Eqs. (1) and (2) no longer apply. We, therefore, adopted the least squares fit procedure outlined in connection with Eqs. (6) and (7) to perform the inversion of the nodal direction $\Sigma_1(\omega)$ ARPES data of Zhang *et al.*[7] In Fig. 4, we present our results of maximum entropy inversion for temperatures $T=128$ and 99 K in the normal state and 35 and 17 K in the superconducting state. In all cases, we get a first estimate for $I^2\chi(\omega)$ from a deconvolution of Eq. (6) using the maximum entropy method. This initial form is parametrized and then a least-squares-fit-like procedure is applied to fit the theoretical $\Sigma_1(\omega)$ values found from finite band Eliashberg theory, Eqs. (A1a)–(A1h), to experiment. The bandwidth is kept at $W=1.2$ eV. All curves show a peak ~65 meV, which is most prominent at 17 K in the superconducting state. As T increases, this peak broadens somewhat and shifts toward higher energies. Besides this resonancelike peak, there is a large, structured background which exists up to 400 meV. It consists of a valley with its lowest point ~115 meV and additional structure beginning at energies ~150 meV. The real part of the self-energy $\Sigma_1(\omega)$ obtained from these spectra after solution of the Eliashberg equations (A1a)–(A1h) is shown in the top frame of Fig. 5. For clarity, we do not show data but in all cases a tight fit was obtained, comparable in quality to the fit shown in the bottom frame of Fig. 3. As it is of considerable interest to compare these results with optics, we present the results of additional calculations in the bottom frame of Fig. 5. Here we used, as in the bottom frame of Fig. 3, for $I^2\chi(\omega)$ the spectra derived from the optical data reported by Hwang *et al.*[5] for a number of temperatures, namely, 300, 200, and 102 K, all in the normal state, and 72 and 27 K in the superconducting state. [The normal state results for $T=27$ K (solid gray line) have also been included for comparison. In all cases, a constant factor of 0.44 was used to go from transport $I^2\chi(\omega)_{\rm tr}$ to quasiparticle $I^2\chi(\omega)$.] A bandwidth of $W=1.6$ eV was chosen to ensure a zero of $\Sigma_1(\omega)$ ~400 meV. The results are very similar as to frequency and temperature variation to those presented in the top frame of Fig. 5. We see, again, a resonancelike structure at ~72 meV, which decays with increasing temperature into a structureless distribution for the real part of the quasiparticle self-energy $\Sigma_1(\omega)$ vs ω at 300 K. It is important to note that the resonance peak is seen even above $T_c\sim 91$ K in both experiments. [A comparison of the superconducting state results for $T=27$ K (black solid line) and the corresponding normal state results (gray solid line) reveals that, here, the resonance peak is at ~62 meV. The gap edge Δ_0 was found to be ~19.2 meV and is responsible for the shift between normal and superconducting states. For a pure *s*-wave gap Δ_0, we would expect this to be Δ_0 but for *d* wave it is less because of the distribution in gap values.]

Finally, we note that in the optics derived case the peaks in the lower temperature curves (72 and 27 K), which are in the superconducting state are more pronounced than they are in the nodal direction ARPES data; however, as we have remarked already, this arises because optics is not momentum resolved. We expect that the coupling to the optical resonance at ~60 meV is larger in the antinodal direction and that our results are likely to be more representative of antinodal direction ARPES data.

In Fig. 6, we compare results for the renormalized energy $E_{\mathbf{k}}$ vs the bare energy $\varepsilon_{\mathbf{k}}$ using the results of our Eliashberg equation solutions based on optics. With $W=1.6$ eV, the crossing is at about 400 meV. For small $\varepsilon_{\mathbf{k}}$, the renormalized

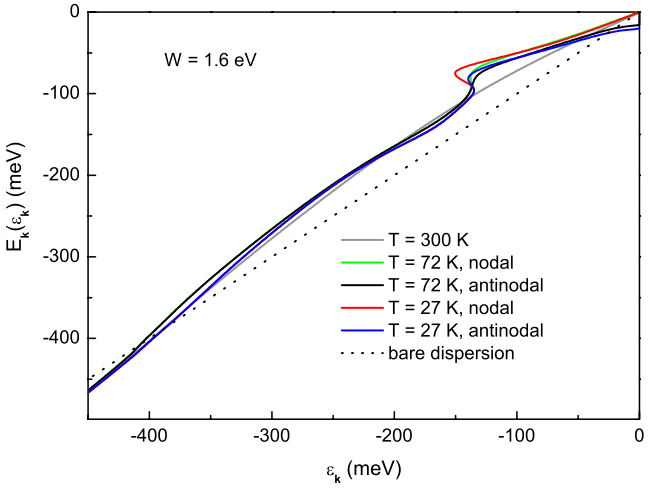

FIG. 6. (Color online) The renormalized dispersion curves $E_{\mathbf{k}}$ im meV as a function of the bare energy $\varepsilon_{\mathbf{k}}$ for various temperatures as labeled. The calculations are based on the spectral densities $I^2\chi(\omega)_{\mathrm{tr}}$ obtained from optics by Hwang *et al.* (Ref. 5) and scaled down by a factor of 0.44. The bandwidth is $W=1.6$ eV. Note that in the superconducting state ($T=72$ K and $T=27$ K), both nodal and antinodal directions are shown.

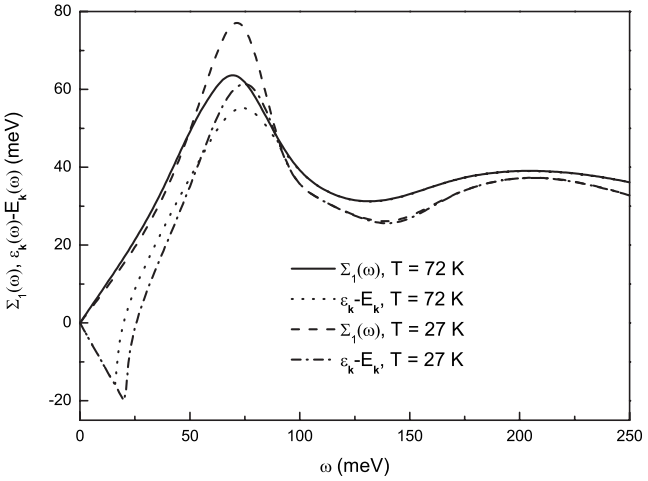

FIG. 7. This illustrates the difference between the self-energy $\Sigma_1(\omega)$ and the quantity $\varepsilon_{\mathbf{k}}-E_{\mathbf{k}}(\omega)$, which are different in the superconducting state, except in the nodal direction.

energy is smaller than its bare value, which corresponds to an increase in effective mass caused by interactions with the medium. This implies band narrowing. By contrast, beyond the zero crossing the renormalized energy is lower than its bare value, which corresponds to band widening. For the infinite band case, the quasiparticle self-energy never crosses zero and becomes small only at $\omega\to\infty$ where bare and interacting dispersion curves meet. There is no concept of band broadening or narrowing in this case. We wish to point out another interesting feature of these curves. For the two low temperature curves (solid lines and dashed lines), we are in the superconducting state and the full Eliashberg equations (A1a)–(A1h) have been solved with the *d*-wave symmetry for the superconducting gap built in. In our formulation, the self-energy $\Sigma(\omega+i\delta)$ is isotropic, although its value does change from its normal state value as the gap opens. It is important to understand that for a superconductor, the quasiparticle energy is given by

$$E_{\mathbf{k}} = \sqrt{\frac{\varepsilon_{\mathbf{k}}^2 + \tilde{\Delta}_1^2(E_{\mathbf{k}})}{Z_1^2(E_{\mathbf{k}})}}, \tag{8}$$

where $\tilde{\Delta}_1(E_{\mathbf{k}})$ and $Z_1(E_{\mathbf{k}})$ are the real parts of the pairing function and of the renormalization function $\omega Z(\omega)=\tilde{\omega}(\omega)$. Thus, at $\varepsilon_{\mathbf{k}}=0$, $E_{\mathbf{k}}=|\tilde{\Delta}(E_{\mathbf{k}})/Z_1(E_{\mathbf{k}})|$. This is zero in the nodal direction as we can see in the two curves of Fig. 6 which are labeled "nodal." For the antinodal direction, $E_{\mathbf{k}}$ at $\varepsilon_{\mathbf{k}}=0$ is no longer zero. (See the two curves in Fig. 6 labeled "antinodal.") Finally, we note that the quasiparticle lifetime $\Gamma(E_{\mathbf{k}})$ in Eliashberg theory is given by

$$\Gamma(E_{\mathbf{k}}) = \frac{E_{\mathbf{k}}Z_2(E_{\mathbf{k}})}{Z_1(E_{\mathbf{k}})} - \frac{\tilde{\Delta}_1(E_{\mathbf{k}})\tilde{\Delta}_2(E_{\mathbf{k}})}{E_{\mathbf{k}}Z_1^2(E_{\mathbf{k}})} \tag{9}$$

and this is not simply the imaginary part of the quasiparticle self-energy in the superconducting state which would be $E_{\mathbf{k}}Z_2(E_{\mathbf{k}})/Z_1(E_{\mathbf{k}})$. Because the paring function is complex, the second term in Eq. (9) is nonzero and this also contributes to the quasiparticle lifetime except in the nodal direction for which $\tilde{\Delta}_{1,2}(E_{\mathbf{k}})=0$. While Eq. (A2) determines the quasiparticle self-energy $\Sigma(\omega)$ in the normal as well as the superconducting state, the equation $\Sigma_1(E_{bfk})=\varepsilon_{\mathbf{k}}-E_{\mathbf{k}}$ can only be used to determine the real part of the quasiparticle self-energy in the normal state and for the nodal direction in the superconducting state. This point is emphasized in Fig. 7 for the optimally doped Bi2212 sample BI96A of Hwang *et al.*[5] with a bandwidth $W=1.6$ eV. We compare in this figure $\Sigma_1(\omega)$ and the difference $\varepsilon_{\mathbf{k}}-E_{\mathbf{k}}(\omega)$ vs ω. In the limit $\omega\to 0$, the $\Sigma_1(\omega)$ curves go to zero, but $\varepsilon_{\mathbf{k}}-E_{\mathbf{k}}(\omega)$ does not in the antinodal direction because there is a finite gap. This gap was already noted in the data of Kordyuk *et al.*[24] The differences are largest at low temperatures. In all cases, the two curves merge at $\omega>100$ meV so that in this region the difference $\varepsilon_{\mathbf{k}}-E_{\mathbf{k}}(\omega)$ does not represent accurately the self-energy in the superconducting state.

IV. SUMMARY AND CONCLUSIONS

Motivated by the appearance of new high precision ARPES data on the real part of the quasiparticle self-energy in Bi2212, we describe a procedure for extracting from this information an electron-boson spectral density $I^2\chi(\omega)$. This work is based on Eliashberg formalism written for a *d*-wave superconducting gap including finite band effects. (The symbol W is used for the bandwidth.) The superconducting state is needed because much of the data available are for temperatures below T_c. Finite bands are needed in order to get renormalized and bare bands to cross. (They would not in an infinite band formalism.) Furthermore, available LDA calculations as well as fits to Fermi surfaces also indicate bands of widths of the order of some eV. In such cases, the final value of the electron-boson spectral density $I^2\chi(\omega)$ from fits to the data is significantly affected by W. While we use a maximum entropy inversion of the convolution integral (6) to get a first

numerical model for the spectral function, in both normal and superconducting states, the Eliashberg equations of the Appendix are employed with a parametrized model for $I^2\chi(\omega)$ and a least squares fit to the data.

In making a comparison with spectral densities obtained from the optical data, it is necessary to recognize that optics involves a momentum average while the ARPES is for a single momentum direction (the nodal direction in our case). Also, the transport $I^2\chi(\omega)_{\rm tr}$ can be different from its quasiparticle counterpart. In making such a comparison, we noted two main differences: One, the transport spectral density is larger in absolute values by a factor of about 2. Second, the resonant peak around 60 meV seen in both spectral densities is more pronounced in optics. We believe this to reflect the importance of the antinodal region not probed in the ARPES data of Zhang *et al.*[7] Other than these differences, there is considerable agreement between the two sets of experimental data giving some evidence that an Eliashberg approach can be used as a phenomenological approach to correlate various data sets.

As is widely done in this field, we interpreted the ARPES data directly as the electron spectral function assuming the so called "matrix element effects" described by Lindroos *et al.*[25] to cause no serious distortion of the spectrum. Furthermore, large inhomogeneities are seen in the scanning tunneling microscopy of the Bi2212 compounds.[26] Although this technique probes only the surface layer, the inhomogeneities could persist in the bulk. Optics is a bulk probe and would average over the inhomogeneities so that our analysis would reflect the average spectral density. The good agreement with ARPES seen here could be taken as evidence that such inhomogeneities, if important, can be treated in an average way. An important contribution to the debate about the mechanism of superconductivity is our finding that the coupling to a high energy background seen in optics is now confirmed in the ARPES data by Zhang *et al.*[7]

ACKNOWLEDGMENTS

Research supported in part by the Natural Sciences and Engineering Research Council of Canada (NSERC) and by the Canadian Institute for Advanced Research (CIFAR). J.P.C. thanks E. J. Nicol and T. Timusk for their interest in this work.

APPENDIX: FINITE BAND *d*-WAVE ELIASHBERG EQUATIONS

The generalization to d wave has already been published by Jiang *et al.*[23] and has been used to describe various aspects of the superconducting state in the cuprates. Here, we include finite bands as well. Assuming particle-hole symmetry for simplicity, the pairs of coupled, nonlinear, clean limit Eliashberg equations take on the following form in an imaginary axis notation:[20]

$$\tilde{\omega}(i\omega_n) = \omega_n + T\sum_m \lambda(m-n)\left\langle \frac{2\tilde{\theta}(i\omega_m,\phi')\tilde{\omega}(i\omega_m)}{\sqrt{\tilde{\omega}^2(i\omega_m)+\tilde{\Delta}^2(i\omega_m,\phi')}}\right\rangle_{\phi'} \tag{A1a}$$

for the renormalized frequencies $\tilde{\omega}(i\omega_n)$ and

$$\tilde{\Delta}(i\omega_n,\phi) = gT\sum_m \cos(2\phi)\lambda(m-n) \times\left\langle \frac{2\tilde{\theta}(i\omega_m,\phi')\tilde{\Delta}(i\omega_m,\phi')\cos(2\phi')}{\sqrt{\tilde{\omega}^2(i\omega_m)+\tilde{\Delta}^2(i\omega_m,\phi')}}\right\rangle_{\phi'} \tag{A1b}$$

for the renormalized pairing potential $\tilde{\Delta}(i\omega_n,\phi) = \tilde{\Delta}(i\omega_m)\cos(2\phi)$. Here, $\omega_n=\pi T(2n+1)$, $n=0,\pm1,\pm2,\ldots$ are the electron Matsubara frequencies, T is the temperature, and $\langle\cdots\rangle_\phi$ denotes the average over the polar angle ϕ of the two-dimensional CuO Brillouin zone. Furthermore, we have

$$\lambda(m-n) = 2\int_0^\infty d\nu \frac{\nu I^2\chi(\nu)}{\nu^2+(\omega_m-\omega_n)^2} \tag{A1c}$$

and for half-filling

$$\tilde{\theta}(i\omega_n,\phi) = \tan^{-1}\left[\frac{W}{2\sqrt{\tilde{\omega}^2(i\omega_n)+\tilde{\Delta}^2(i\omega_n,\phi)}}\right]. \tag{A1d}$$

We assumed here, for simplicity, that the same form of $I^2\chi(\omega)$ holds for the $\tilde{\omega}$ and the $\tilde{\Delta}$ channel, Eqs. (A1a) and (A1b), respectively, and the numerical factor g was introduced to account for the fact that the projection of the general electron-boson spectral density will, in general, be different in the two channels. This factor g can be determined from the linearized equations (A1a) and (A1b), which are valid at $T=T_c$ whenever T_c and $I^2\chi(\omega)$ are known. In our particular case studied here, $g\sim1$.

These equations are then to be analytically continued using a method formulated by Marsiglio *et al.*[21] and we get the following result on the real ω axis:

$$\begin{aligned}\tilde{\omega}(\omega) = \omega + iT\sum_{m=0}^{\infty}[\lambda(\omega-i\omega_m)-\lambda(\omega+i\omega_m)] \\ \times\left\langle \frac{2\tilde{\theta}(i\omega_m,\phi')\tilde{\omega}(i\omega_m)}{\sqrt{\tilde{\omega}^2(i\omega_m)+\tilde{\Delta}^2(i\omega_m,\phi')}}\right\rangle_{\phi'} \\ + i\int_{-\infty}^{\infty} dz I^2\chi(z)[n(z)-f(z-\omega)] \\ \times\left\langle \frac{2\tilde{\theta}(\omega-z)\tilde{\omega}(\omega-z+i\delta)}{\sqrt{\tilde{\omega}^2(\omega-z+i\delta)-\tilde{\Delta}^2(\omega-z+i\delta,\phi')}}\right\rangle_{\phi'}\end{aligned} \tag{A1e}$$

for the fully renormalized frequencies $\tilde{\omega}(\omega)$ and

$$\tilde{\Delta}(\omega,\phi) = gT\sum_{m=0}^{\infty} \cos(2\phi)[\lambda(\omega - i\omega_m) + \lambda(\omega + i\omega_m)] \times \left\langle \frac{2\tilde{\theta}(i\omega_m,\phi')\tilde{\Delta}(i\omega_m,\phi')\cos(2\phi')}{\sqrt{\tilde{\omega}^2(i\omega_m) + \tilde{\Delta}^2(i\omega_m,\phi')}} \right\rangle_{\phi'} + ig\int_{-\infty}^{\infty} dz \cos(2\phi) I^2\chi(z)[n(z) - f(z-\omega)] \times \left\langle \frac{2\tilde{\theta}(\omega - z)\tilde{\Delta}(\omega - z + i\delta,\phi')\cos(2\phi')}{\sqrt{\tilde{\omega}^2(\omega - z + i\delta) + \tilde{\Delta}^2(\omega - z + i\delta,\phi')}} \right\rangle_{\phi'} \tag{A1f}$$

for the fully renormalized pairing potential $\tilde{\Delta}(\omega,\phi)$ on the real axis. Here, the function $\tilde{\theta}(\omega,\phi)$ is defined as

$$\tilde{\theta}(\omega,\phi) = \tan^{-1}\left[\frac{iW}{2\sqrt{\tilde{\omega}^2(\omega) - \tilde{\Delta}^2(\omega,\phi)}}\right] \tag{A1g}$$

and

$$\lambda(\omega) = \int_{-\infty}^{\infty} d\nu \frac{I^2\chi(\nu)}{\nu - \omega + i\delta}. \tag{A1h}$$

Note that in cases where the square root is complex, the branch with a positive imaginary part is to be chosen.

For the normal state only, Eq. (A1a) remains with $\tilde{\Delta}(i\omega_n,\phi) \equiv 0$, which is then analytically continued to the real axis again using Eq. (A1e) with $\tilde{\Delta}(\omega,\phi)$ set equal to zero. The quasiparticle self-energy is calculated using the relation

$$\Sigma(\omega) = \omega - \tilde{\omega}(\omega), \tag{A2}$$

which is valid in the normal as well as in the superconducting state.

*schachinger@itp.tu-graz.ac.at; URL: www.itp.tu-graz.ac.at/~ewald

[1] E. Schachinger, D. Neuber, and J. P. Carbotte, Phys. Rev. B **73**, 184507 (2006).

[2] J. P. Cabotte and E. Schachinger, Ann. Phys. (Leipzig) **15**, 585 (2006).

[3] Junren Shi, S.-J. Tang, Biao Wu, P. T. Sprunger, W. I. Yang, V. Brouet, X. J. Zhou, Z. Hussain, Z.-X. Shen, Zhenyu Zhang, and E. W. Plummer, Phys. Rev. Lett. **92**, 186401 (2004).

[4] X. J. Zhou, J. Shi, T. Yoshida, T. Cuk, W. L. Yang, V. Brouet, J. Nakamura, N. Mannella, S. Komiya, Y. Ando, F. Zhou, W. X. Ti, J. W. Xiong, Z. X. Zhao, T. Sasagawa, T. Kakeshita, H. Eisaki, S. Uchida, A. Fujimori, Z. Zhang, E. W. Plummer, R. B. Laughlin, Z. Hussain, and Z.-X. Shen, Phys. Rev. Lett. **95**, 117001 (2005).

[5] J. Hwang, T. Timusk, E. Schachinger, and J. P. Carbotte, Phys. Rev. B **75**, 144508 (2007).

[6] A. S. Mishchenko and N. Nagaosa, Phys. Rev. Lett. **93**, 036402 (2004).

[7] Wentao Zhang, Guodong Liu, Lin Zhao, Haiyun Liu, Jianqiao Meng, Xiaoli Dong, Wei Lu, J. S. Wen, Z. J. Xu, G. G. Gu, T. Sasagawa, Guiling Wang, Yong Zhou, Hongbo Zhang, Yong Zhou, Xiaoyang Wang, Zhongxian Zhao, Cuangtian Chen, Zuyan Xu, and X. J. Zhou, arXiv:0711.1706 (unpublished).

[8] R. S. Markiewicz, S. Sahrakorpi, M. Lindroos, Hsin Lin, and A. Bansil, Phys. Rev. B **72**, 054519 (2005).

[9] A. Knigavko and J. P. Carbotte, Phys. Rev. B **72**, 035125 (2005); **73**, 125114 (2006).

[10] E. Cappelluti and L. Pietronero, Phys. Rev. B **68**, 224511 (2003).

[11] W. Meevasana, X. J. Zhou, S. Sahrakorpi, W. S. Lee, W. L. Yang, K. Tanaka, N. Mannella, T. Yoshida, D. H. Lu, Y. L. Chen, R. H. He, Hsin Lin, S. Komiya, Y. Ando, F. Zhou, W. X. Ti, J. W. Xiong, Z. X. Zhao, T. Sasagawa, T. Kakeshita, K. Fujita, S. Uchida, H. Eisaki, A. Fujimori, Z. Hussain, R. S. Markiewicz, A. Bansil, N. Nagaosa, J. Zaanen, T. P. Devereaux, and Z.-X. Shen, Phys. Rev. B **75**, 174506 (2007).

[12] J. Hwang, T. Timusk, and G. D. Lu, J. Phys.: Condens. Matter **18**, 125208 (2007); Nature (London) **427**, 714 (2004).

[13] E. Schachinger, J. J. Tu, and J. P. Carbotte, Phys. Rev. B **67**, 214508 (2003).

[14] A. S. Aleksandrov, V. N. Grebenev, and E. A. Mazur, Pis'ma Zh. Eksp. Teor. Fiz. **45**, 357 (1987).

[15] S. Verga, A. Knigavko, and F. Marsiglio, Phys. Rev. B **67**, 054503 (2003).

[16] F. Dogan and F. Marsiglio, Phys. Rev. B **68**, 165102 (2003).

[17] B. Mitrović and J. P. Carbotte, Can. J. Phys. **61**, 758 (1983); **61**, 789 (1983).

[18] C. Grimaldi, E. Capelluti, and L. Pietronero, Europhys. Lett. **42**, 667 (1998).

[19] E. Cappelluti, C. Grimaldi, and L. Pietronero, Phys. Rev. B **64**, 125104 (2001).

[20] Han-Yong Choi, Phys. Rev. B **53**, 8591 (1996).

[21] F. Marsiglio, M. Schossmann, and J. P. Carbotte, Phys. Rev. B **37**, 4965 (1988).

[22] F. Marsiglio, Phys. Rev. B **45**, 956 (1992).

[23] C. Jiang, E. Schachinger, J. P. Carbotte, D. N. Basov, and T. Timusk, Phys. Rev. B **54**, 1264 (1996).

[24] A. A. Kordyuk, S. V. Borisenko, V. B. Zabolotnyy, J. Geck, M. Knupfer, J. Fink, B. Büchner, C. T. Lin, B. Keimer, H. Berger, A. V. Pan, Seiki Komiya, and Yoichi Ando, Phys. Rev. Lett. **97**, 017002 (2006).

[25] M. Lindroos, S. Sahrakorpi, and A. Bansil, Phys. Rev. B **65**, 054514 (2002).

[26] J. Lee, K. Fujita, K. McElroy, J. A. Slezak, M. Wang, Y. Aiura, V. Bando, H. Ishikado, T. Masui, J. X. Zhu, H. V. Balatsky, H. Eisaki, S. Uchida, and J. C. Davis, Nature (London) **442**, 546 (2006).